Three-dimensional modeling of tracers in the deep Pacific Ocean
II. Radiocarbon and the circulation

by Manuel E. Fiadeiro[1]

ABSTRACT

The radiocarbon data from the *GEOSECS* Pacific expedition was used to test the abyssal circulation model presented in part I of this series. The results show that a uniform increase of the upwelling rate from the bottom to the top of the model cannot explain the qualitative features of the radiocarbon distribution. A new model is presented in which the upwelling rate attains a maximum between the Bottom and Deep Water. The qualitative features of the distributions are well reproduced including an enchancement of the vertical gradients in the southwest region of the Pacific (the benthic front). The implication is that zonal gradients of density are the next most important feature to include in models of the thermohaline circulation. This model gives approximately 700 years for the residence time of the water in the deep Pacific basin.

1. Introduction

One of the most important aspects of modeling tracers in the abyssal ocean is to test hypotheses concerning the thermohaline circulation. In a previous paper (Fiadeiro and Craig, 1978) we tested the Stommel and Arons model of the abyssal circulation (Stommel and Arons, 1960) on the three-dimensional distributions of salinity and oxygen in the deep Pacific Ocean. The deep ocean was assumed to consist of a homogeneous layer from 1 to 4 km and the upwelling velocity was assumed to increase or decrease uniformly from a value of zero at the bottom to a value at the base of the thermocline, the top of the model, which can be a function of latitude and longitude or a constant. The resulting velocity field represents the barotropic mode of the circulation.

We showed that the model with a horizontally uniform upwelling gave the most reasonable solutions for the distributions of salinity and oxygen over most of the Pacific. I shall refer henceforth to this model as 3DM/I. The worst fit was found in the southwestern region, where the benthic front (Craig *et al.*, 1972) is bounded above by water with characteristics of the Central Pacific and below by water with Antarctic Circumpolar characteristics. Succeeding calculations for nitrate, phosphate,

1. Department of Geology and Geophysics, Yale University, New Haven, Connecticut, 06511, U.S.A.

silicate and alkalinity showed the same discrepancies in this region. The model solutions did not reproduce the benthic front features, even qualitatively.

The nonconservative tracers were fitted with a source (or sink) function which allows for variation with depth. For simplicity, we chose to parameterize the source term as an exponential function of depth because it is the simplest function (only two parameters) which does not change sign. With model 3DM/I the oxygen sink and the phosphate, nitrate and oxidative carbon sources decrease downward with a typical length scale of 1 km while the silicate and alkalinity sources decrease with a length scale of 2 kms. The major difference between these two classes of tracers, a shallow (1.2 km) maximum or minimum deepening toward the west in the former and a deep (2.5 km) maximum concentrated in the east for the latter, is adequately explained in the model by the difference between the depth scales of their respective source functions.

In a previous paper (Fiadeiro, 1980) I noted that the distributions of alkalinity and silicate at their maximum suggest an anticyclonic motion for the Deep Water. To produce this pattern of circulation, vorticity conservation requires that dw/dz (w') be negative in this region. This being the case, the upwelling velocity should increase up to a maximum value at mid-depth producing the cyclonic type of circulation of model 3DM/I in the bottom layer and then decrease toward the base of the thermocline.

It is not yet clear at which depth the vertical motion vanishes, but somewhere it must change sign to match the downwelling at the bottom of the Ekman layer in subtropical regions where the curl of the wind stress is negative. With a decreasing upwelling in the deep layer the horizontal circulation becomes anticyclonic, feeding the excess water to the western boundary current which then flows southward.

These features were incorporated into a new model, 3DM/II, presented here. The main interest of these calculations is to show the zero order effects of baroclinity on the tracer distributions. Zonal gradients of density produce a change of w' with depth and we want to find if this effect is important. The model assumes two homogeneous layers, each with a constant value of w'. In the bottom layer w' is positive; in the deep layer w' can be positive, negative or zero. The relative change in w' is estimated by trying to reproduce the typical features of the C-14 distribution.

2. The carbon-14 in the deep Pacific

The C-14/C-12 ratio in the water is not a tracer but behaves much like a radioconservative tracer. If C denotes the concentration of total dissolved inorganic carbon, J the respective source term, R the C-14/C-12 ratio in the water relative to a standard and R_J the corresponding ratio in the source term, then we have

$$D[C] = \frac{\partial C}{\partial t} - \nabla \cdot (K \cdot \nabla C - VC) = J \tag{1}$$

for total carbon and

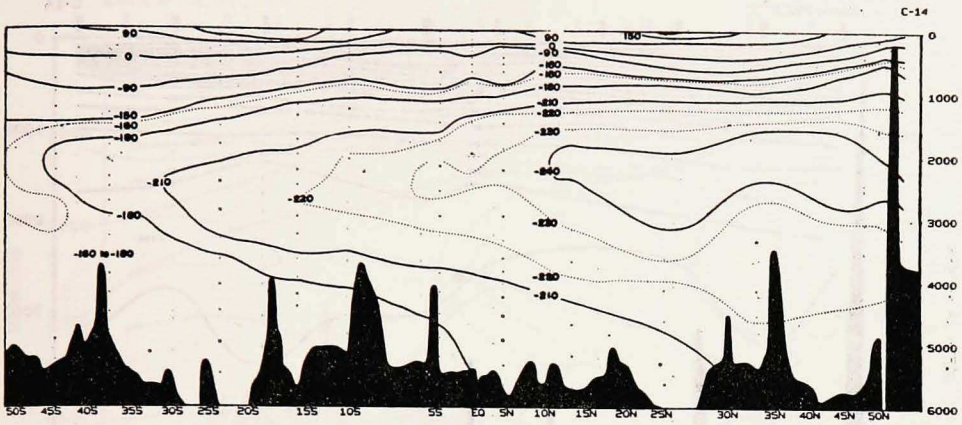

Figure 1. The NS vertical section of ΔC^{14} (in ‰) around 180W (from Ostlund and Stuiver, 1980).

$$D[RC] = -\lambda RC + R_J J \tag{2}$$

for carbon-14. Multiplying Eq. 1 by R and substituting in Eq. 2,

$$C \cdot D[R] = -C \cdot \lambda R + (R_j - R)J - 2[\nabla C \cdot K \nabla R] \tag{3}$$

or

$$D[R] = -\lambda R + (R_j - R)J/C - 2[\nabla \ln C \cdot K \cdot \nabla R] \quad . \tag{4}$$

The first term on the r.h.s. is of the order of 10^{-4}. The second term is less than 10% of the first for the oldest Pacific water and the largest contribution to the third term comes from the vertical component of the gradients and is of the order of 10^{-6}. So, as a first approximation the relative C-14 ratio can be used as a radioconservative tracer as was done by Munk (1966) and Kuo and Veronis (1973). The other alternative, to work with the absolute values of C-14 as a radiononconservative tracer, subjects the values to the errors of both the total carbon and C-14. For the GEOSECS data, the error relative to the total variation in C-14 is smaller than for total carbon and it seems preferable not to include the uncertainty of the carbon determination on the C-14 distribution.

The GEOSECS Pacific C-14 data is given by Ostlund and Stuiver (1980). Their vertical sections are reproduced in Figures 1, 2, 3. C-14 has a characteristic minimum at the core of the Pacific Deep Water. The vertical gradient between the Deep and Bottom Waters is greater in the western section (Fig. 1) than in the eastern section (Fig. 3). While in the western section a pronounced minimum spreads south over the benthic front, the Deep Water in the eastern section shows gentler vertical gradients.

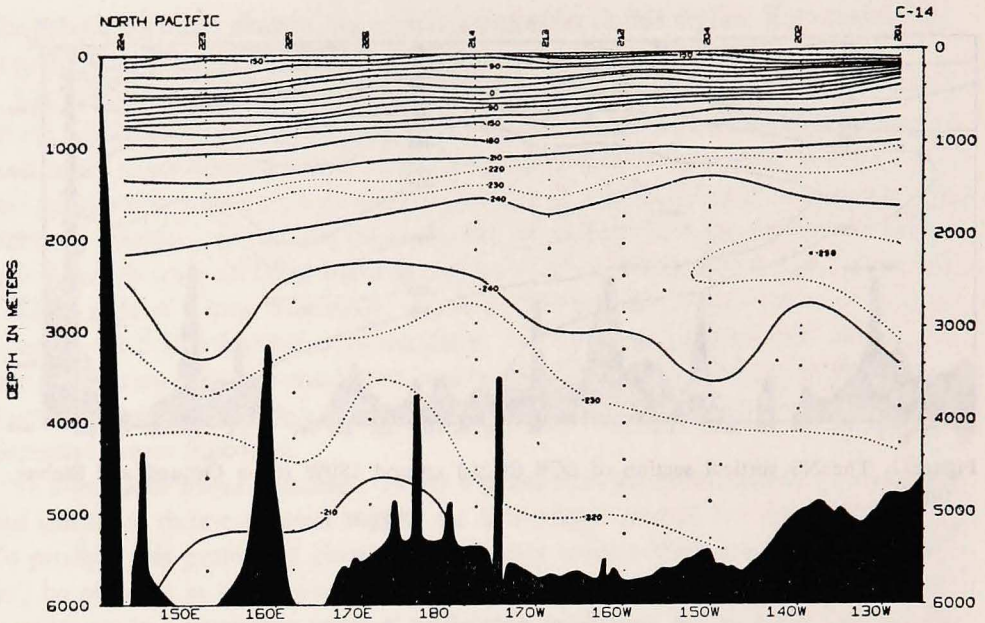

Figure 2. The EW vertical section of ΔC^{14} (in ‰) around 32N (from Ostlund and Stuiver, 1980).

The values reach an absolute minimum in the Deep Water at a depth between 2 and 2.5 km. At 30N (Fig. 2) the minimum reaches values less than −250‰ on the eastern side and the 240‰ isolines extend across the section with a general tendency to diverge eastward. The Bottom Water at St. 226 (171W) has values higher than the adjacent stations by 5 to 10‰. It is the "youngest" water entering the North Pacific basin.

The vertical profiles in the Circumpolar have an almost constant value of −163‰ below 2 km. Bottom water with this value enters the Pacific around Chatham Rise and changes relatively little in the southwestern Pacific. Vertical mixing with the Deep Water above is restricted to the erosion of the top of the water mass producing the enhanced gradient typical of the benthic front. Figure 4 shows the horizontal distribution of C-14 at 4 km. North of the Tokelau Passage the Bottom Water loses C-14 by decay and by mixing with the Deep Water, reaching a minimum in the northeastern region of the Pacific. The general strike of the isolines, NW-SE in the South Pacific rotating to a more W-E direction in the North Pacific is reminiscent of the other tracers and is a characteristic feature for the tracers with a cyclonic bottom circulation (Kuo and Veronis, 1973; Fiadeiro and Craig, 1978).

The spreading of new (bomb-produced) C-14 follows the Arctic and Antarctic Intermediate Waters. The distribution under 1 km, with the possible exception of

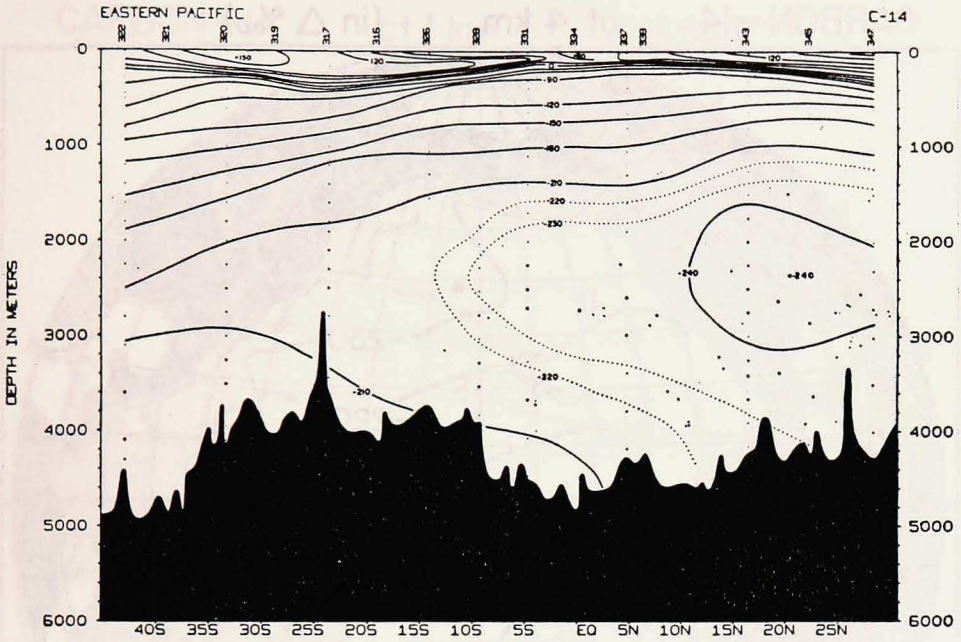

Figure 3. The NS vertical section of ΔC^{14} (in ‰) around 120W (from Ostlund and Stuiver, 1980).

the middle regions of the tropical gyres where the thermocline is deeper, has probably not yet been significantly disturbed as is indicated by the tritium profiles (Ostlund *et al.*, 1979). The distribution at 1 km is shown in Figure 5 and will be taken as indicative of the conditions prior to C-14 injection into the environment.

The western section of the GEOSECS Pacific salinity data is shown in Figure 6. Other sections were presented in the first paper of this series and are not essential for the discussion to follow.

3. The model solutions

For the C-14 boundary conditions, a composite vertical profile of GEOSECS stations 290 and 293 was used for the western boundary and of stations 76 and 78 for the eastern boundary of the Circumpolar Current. The values at the top boundary were taken from the 1 km distribution shown in Figure 5.

The solutions presented here were obtained using the weighted-mean scheme of Fiadeiro and Veronis (1977) which gives a better approximation than the one used in the previous paper (part I). Otherwise, the same approach was followed.

A typical solution of model 3DM/I is presented in Figure 7. In Figure 7a are shown, anticlockwise from the top, the 4 km, the Circumpolar and the western

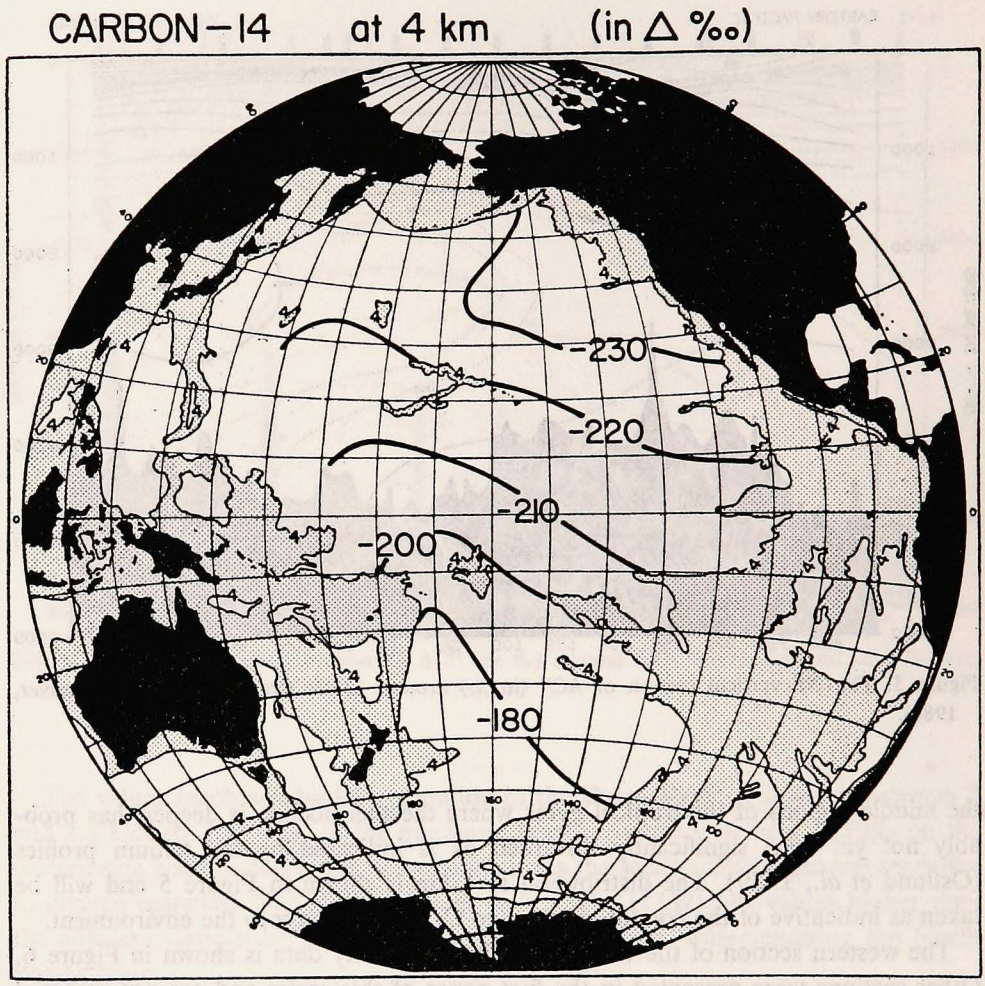

Figure 4. The distribution of ΔC^{14} at 4000 m.

boundary sections. In Figure 7b, the 2.5 km, a W-E section at 35N and a N-S section 60E from the western boundary are illustrated. The model solutions can be compared with the observed distributions in Figures 1, 2, 3 and 4 taking into account the geometric distortion produced by straightening the boundaries of the North Pacific (in the South Pacific the model represents the area between 90W and 180W, but the North Pacific boundary at 50N should correspond to the longitudes between 130W and 140E).

It is clear that model 3DM/I cannot reproduce most of the features of the C-14 distribution. The solution has the minimum at the bottom. The water "ages" from the southwest to the northeast without much depth variation below 2.5 km (see up-

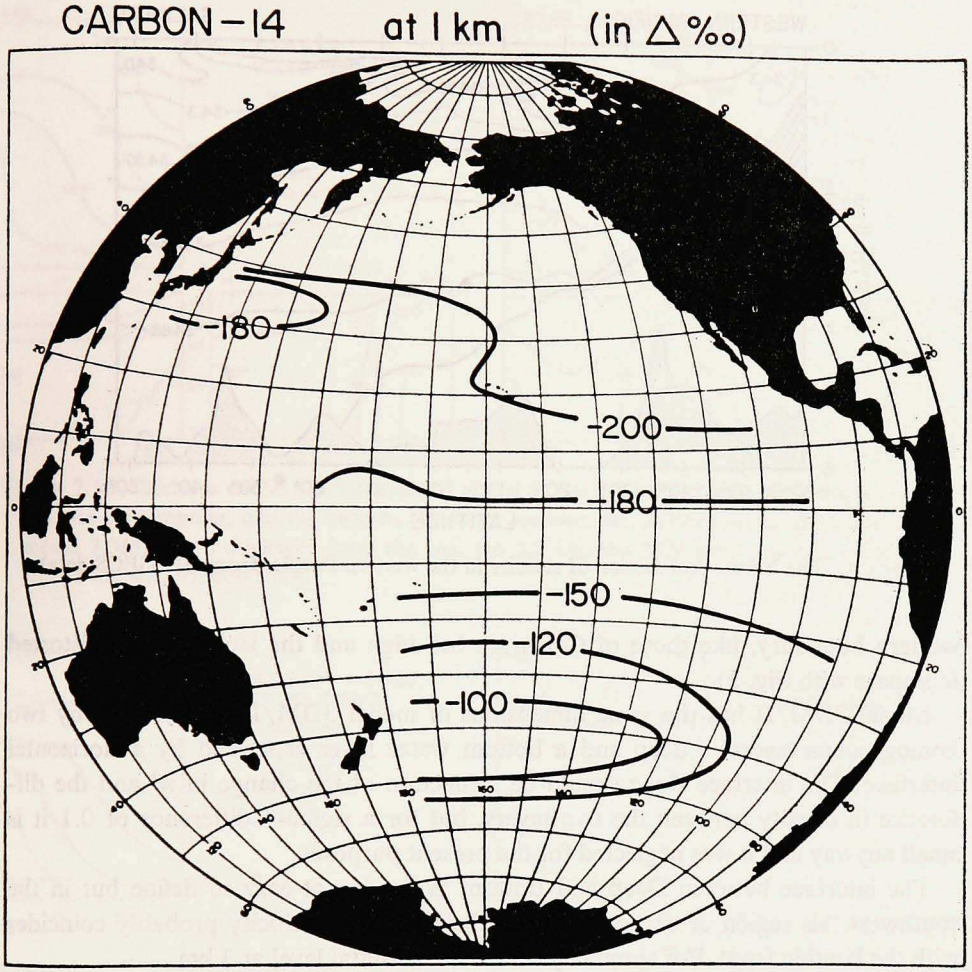

Figure 5. The distribution of ΔC^{14} at 1000 m.

per left sections of Figs. 7a and 7b). The values in the western boundary (lower right of Fig. 7a) are too high (> −180‰) up to 20N. The southern portion of the section is clearly dominated by the Circumpolar profile at all levels. The influence of the upper boundary is felt down to about 2 km and appears to be artificially imposed on the interior solution. The absolute values can be changed by varying a scaled decay constant but the pattern remains.

The salinity solution of this model is shown in Figures 8a and 8b. Except for the western boundary (lower right of Fig. 8a), the distribution is not entirely unreasonable. The effect of divergence or convergence in the interior solution is not great because the distribution is mostly vertically stratified. However, the values at the

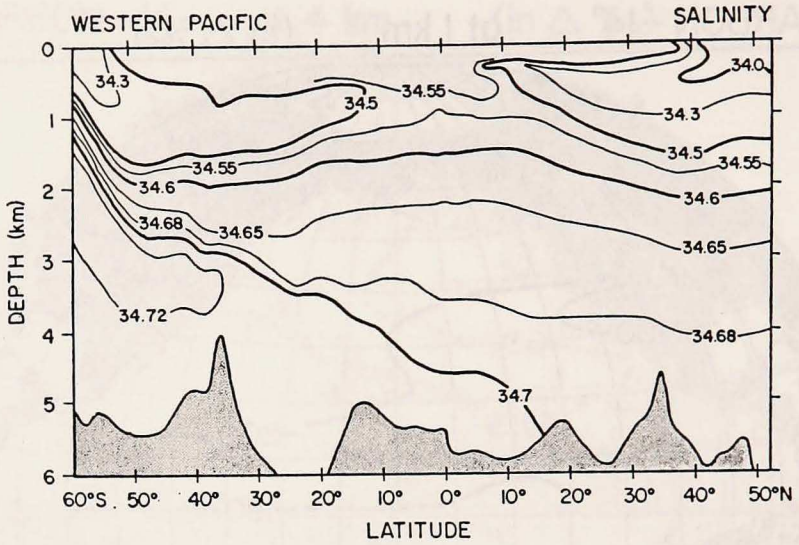

Figure 6. The NS vertical section of salinity in the western Pacific (from GEOSECS data).

western boundary, like those of C-14, are too high and the isolines very distorted (compare with Fig. 5).

Model 3DM/II has the same dimensions of model 3DM/I. It is formed by two homogeneous layers, a deep and a bottom water layer separated by a horizontal interface. The interface slope should be a function of the change in w' and the difference in density between the two layers, but for a sigma-4 difference of 0.1 it is small anyway and it was neglected for the present purposes.

The interface between Deep and Bottom Water is not easy to define but in the southwest this region of vertical shear in the horizontal velocity probably coincides with the benthic front. For simplicity I took a horizontal level at 3 km.

The two layers can in principle have different values for the four parameters K_v, K_h, w' and R but it would be irrelevant to fit eight parameters to two conservative tracers. The purpose of the model is to estimate the effect of the circulation on the general features of the tracer distributions rather than to obtain a detailed reproduction of the oceanographic data.

The Circumpolar Current is very crudely represented in this model. It extends from 50 to 60S with a no flux condition at its southern boundary. R represents the flux of water through the Drake Passage and was fixed at 10 Sv per km depth for both layers. The effect of R on the interior distribution is slight and serves mainly to maintain a smooth change in the Circumpolar values from one boundary to the other. No strict physical significance should be given to the value of R.

The vertical and horizontal eddy diffusion coefficients are assumed to be constant. I will discuss then, the effect on the solutions of four parameters: the horizontal and

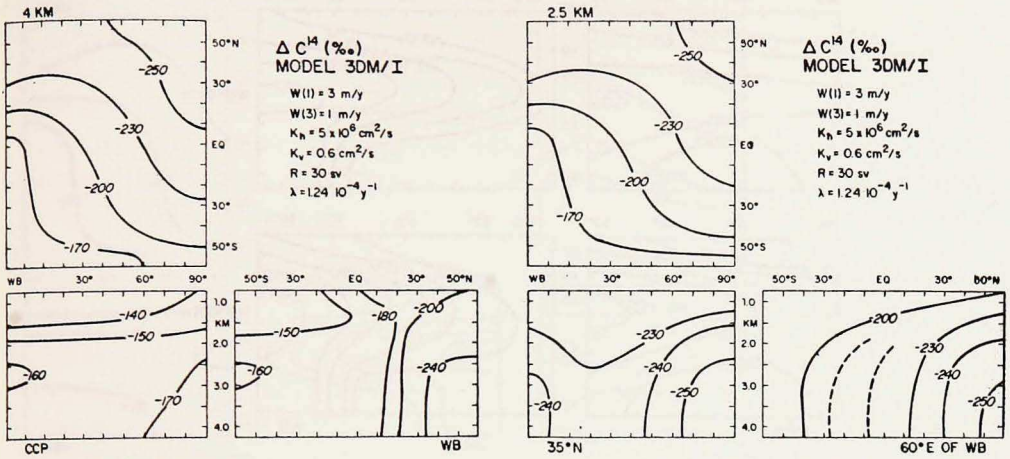

Figure 7. (a) Sections of the ΔC^{14} solution of model 3DM/I. Anticlockwise from the top, the 4 km, the Circumpolar, and the western boundary sections. (b) Sections of the ΔC^{14} solution of model 3DM/I. Anticlockwise from the top, the 2.5 km, the 35N section and a section 60° east of the western boundary.

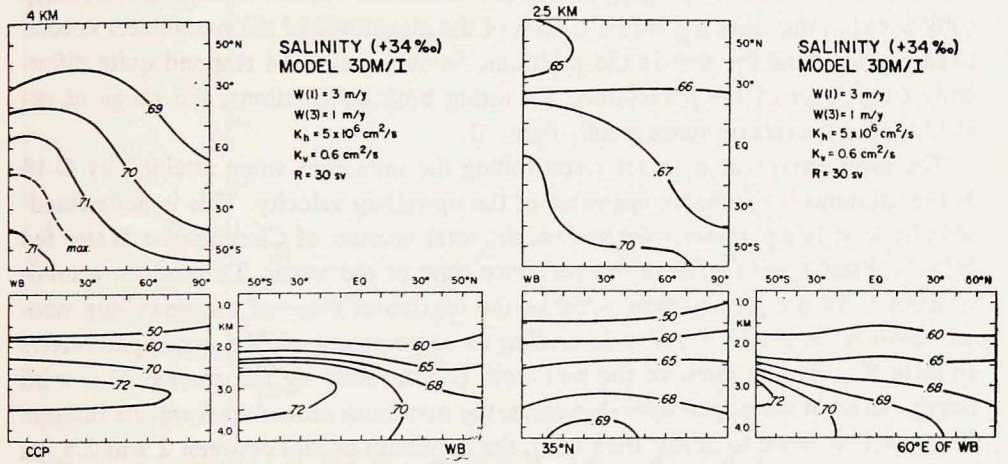

Figure 8. (a) Salinity solution of model 3DM/I. Same sections as in Figure 7a. (b) Salinity solution of model 3DM/I. Same sections as in Figure 7b.

vertical eddy diffusion coefficients (K_v and K_h), the upwelling velocity at the interface between the deep and bottom layers $w(3)$, and at 1 km $w(1)$, the top of the model.

The relevant features the model tries to reproduce are: the minimum value attained by C-14, its depth and horizontal spreading, the overall N-S and E-W gradi-

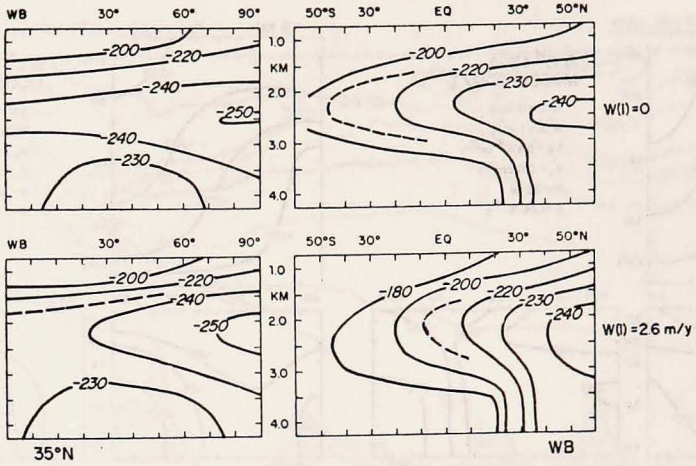

Figure 9. The WE sections at 35N and the western boundary sections of the 3DM/II model solutions of ΔC^{14} for $w(1) = 0$ and $w(1) = w(3)$.

ents of C-14 and salinity in the Bottom Water and at the C-14 minimum, and the enhancement of the vertical gradients in the southwest Pacific. The fits are certainly subjective but they give a good indication of the magnitude of the parameters needed to reproduce these features in the solutions. Salinity and C-14 respond quite differently to changes of the parameters. By fitting both distributions, the range of acceptable parameters becomes greatly reduced.

The most important parameter controlling the minimum value attained by C-14 in the solutions is the maximum value of the upwelling velocity. This is understandable because this parameter determines the total amount of Circumpolar Water fed into the Pacific and therefore the residence time of the water. To produce a minimum of C-14 not greater than −250‰, the maximum value of the upwelling velocity must be around 2.5 m/y, depending to some extent on the other parameters (mainly K_h). The position of the minimum is controlled by the change of w with depth. As w' in the upper layer decreases, the minimum moves up from the bottom. When $w(1)$ is equal to or less than $w(3)$, the minimum occurs between 2 and 2.5 km as in the real distribution.

The next most important parameter is K_v. The ratio between the vertical advection and diffusion controls the salinity lost by the bottom water and the gradient in C-14 between the deep and bottom water.

The salinity at the bottom of GEOSECS St. 218 (50°27′N, 176°35′W) is not more than 34.688‰ and the only way for the bottom water to lose salt is by vertical diffusion. Fixing $w(3) = 2.6$ m/y and requiring that the salinity at the bottom of the North Pacific be less than 34.69‰ establishes a correlation between K_v and $w(1)$. If $w(1) = 0$ the minimum K_v is 0.6 cm²/s, if $w(1) = 1/2\ w(3)$, then $K_v = 0.7$ cm²/s

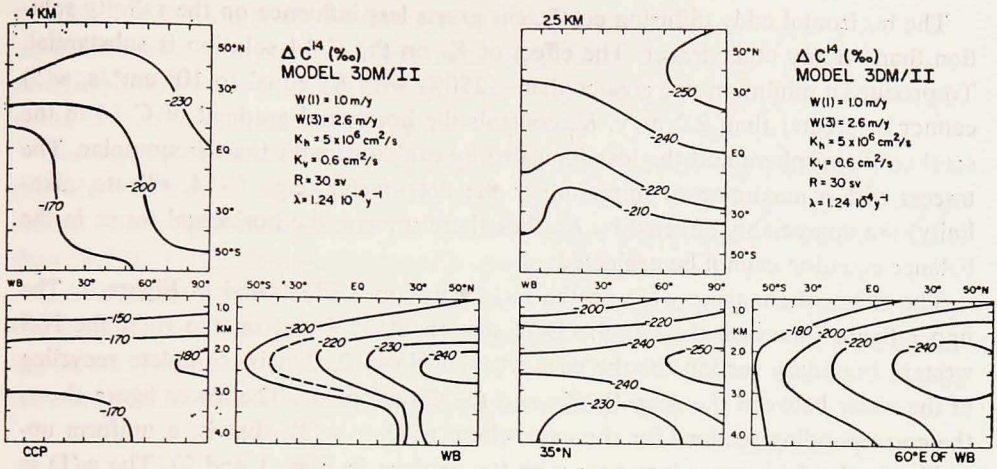

Figure 10. (a) ΔC^{14} solution of model 3DM/II. Same sections as in Figure 7a. (b) ΔC^{14} solution of model 3DM/II. Same sections as in Figure 7b.

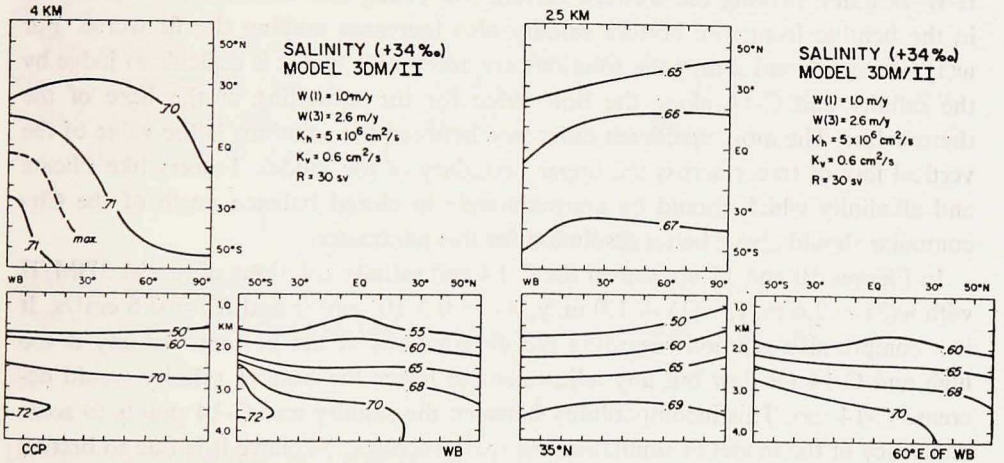

Figure 11. (a) Salinity solution of model 3DM/II. Same sections as in Figure 7a. (b) Salinity solution of model 3DM/II. Same sections as in Figure 7b.

and for $w(1) = w(3)$, $K_v = 0.8$ cm²/s. These values are almost independent of the value of K_h.

The gradient of C-14 between the minimum and the bottom is also a function of K_v. To produce a difference of 15‰ in C-14, K_v cannot be greater than 0.5 cm²/s. Salinity and C-14 thus show different tendencies for the ratio of vertical diffusion to advection. While salinity requires a higher ratio for the bottom water to lose salt, C-14 requires a lower ratio to produce the observed deep to bottom gradient.

The horizontal eddy diffusion coefficient exerts less influence on the salinity solution than on any other tracer. The effect of K_h on the C-14 solution is substantial. To produce a minimum not greater than $-250‰$ with K_h equal to 10^7 cm^2/s, $w(3)$ cannot be greater than 2.2 m/y. K_h controls the horizontal gradient of C-14 in the southern hemisphere and the loss (or gain) by exchange with the Circumpolar. The tracers with a maximum or minimum in the deep water (e.g., C-14, silicate, alkalinity) are appreciably affected by K_h. For these tracers, the horizontal terms in the balance equation cannot be neglected.

The effect of changing $w(1)$ on the C-14 solution is illustrated in Figure 9. The upper figure shows on the left the E-W section at 35N and on the right the N-S western boundary section for the case where $w(1) = 0$, that is, complete recycling of the water between the deep Pacific and the Circumpolar. The lower figure shows the corresponding sections for the case where $w(1) = w(3)$, that is, a uniform upwelling in the deep water (compare with the sections in Figs. 1 and 2). The $w(1) = 0$ solution gives values that are too low in the top km and in the western boundary; it produces a very sharp maximum at 2.5 km. This seems to preclude downwelling at the base of the thermocline. A uniform upwelling in the deep water enhances the E-W variation making the western section too young and attenuates the gradients in the benthic front; the bottom salinity also increases making the fit worse. For $w(1)$ between 1 and 2 m/y the solutions are acceptable and it is difficult to judge by the salinity and C-14 alone the best value for the upwelling at the base of the thermocline. The most significant difference between the solutions is the value of the vertical flux of tracer across the upper boundary of the model. Tracers like silicate and alkalinity which should be approximately in closed balance north of the Circumpolar should give a better resolution for this parameter.

In Figures 10 and 11 are shown the C-14 and salinity solutions of model 3DM/II with $w(3) = 2.6$ m/y, $w(1) = 1.0$ m/y, $K_h = 0.5\ 10^7$ cm^2/s and $K_v = 0.6$ cm^2/s. It is a compromise solution regarding the distributions at the bottom. Salinity is too high and C-14 too low but any adjustment to lower the bottom salinity would decrease C-14 too. This incompatibility between the salinity and C-14 points to some deficiency of the model in simulating the real processes. I believe it is due to bottom topography. The western basin is deeper than the eastern by about 1 km. Values of C-14 greater than $-210‰$ penetrate up to 30N on the western side near the bottom (Fig. 1).

The C-14 solution at 2.5 km shows a displacement of the minimum value ($< -250‰$) toward lower latitudes. In the real distribution this seems to occur even at 4 km, but without measurements north of 32N and east of 170W it is difficult to judge what really happens. Most of the features are nevertheless quite well reproduced. In particular the strong vertical gradients near the western boundary with the penetration of a tongue of $-220‰$ water to 20S shows clearly in the solution (lower right of Fig. 10a and Fig. 1). The solution shows also the rounded profiles with a

minimum at 2.5 km in the eastern Pacific (lower right of Fig. 10b and Fig. 3). The north vertical section has the same general form of the observed distribution, namely an aging of the water from the bottom to the deep with the minimum around 2.5 km at the eastern side (lower left of Fig. 10b and Fig. 2).

The vertical structure of the salinity solution also shows improvement although the values at the bottom are a little too high. The greatest difference is in the western section (lower right of Fig. 11a). The erosion of the water tongue with salinity greater than 34.72‰ by the benthic front is now clearly seen.

It is interesting to note that the distribution of density will have a similar qualitative pattern. The eastward fanning of the isolines from a depth of 3 km is conspicuous in the South Pacific across the benthic front. It is this effect that will produce the change in w' with depth which we tried to estimate here.

4. Conclusions

The main purpose of this paper is to show the radical difference in the model solutions of C-14 produced by a change of dw/dz with depth. It is clear that baroclinity is an important feature and must be included in models of the thermohaline circulation.

The pressure differences that drive the thermohaline circulation are extremely small compared with those of the wind-driven circulation. With a horizontal length scale $L = 6000$ km for the ocean basin, $H = 1$ km for the vertical scale, $f = 10^{-4}$, $\beta = 2.10^{-13}$, $w = 10^{-5}$ cm/s and

$$V = \frac{\Delta p}{f\rho L} = \frac{f}{\beta}\frac{w}{H}, \quad \Delta p = \frac{f^2}{\beta}\frac{wL}{H},$$

the value of Δp is 3000 dynes/cm^2 or 3 cm of water across the basin.

The difference in density needed to cause the vertical velocity to vanish is

$$\Delta\rho = \frac{\rho f^2}{g\beta}\frac{w}{H^2}$$

i.e., $\Delta\rho = 3.10^{-5}$gr/cm^3 or .03 units in sigma-4.

Clearly these values are possible with the observed distributions. The wind-driven circulation produces a western deepening of the thermocline causing a deficiency of density at the top of the deep water. The bottom western boundary current brings an excess of density to the bottom. The vertical gradient of density in the deep water is thus greater in the western than in the eastern side of the ocean. Apparently by 3 km, the pressure field created by the wind-driven circulation is completely compensated by the baroclinity of the deep ocean. This implies that the pressure field produced by the wind and the effects of lateral and bottom boundary conditions are also important features in the thermohaline circulation.

The model indicates that the abyssal (deep and bottom water) and surficial (sur-

face and intermediate water) circulations are somewhat uncoupled by the thermal structure of the ocean. Wyrtki (1961) proposed a model of the thermohaline circulation in which these two components of the circulation were essentially independent. His model was zonally integrated with flow along isopycnals and his circulation could not be closed with symmetrical conditions along the equator. However, the idea of some separation between the two components resulting in a four-layer circulation seems to apply.

According to model 3DM/II about 8 Sv of Bottom Water upwell to form Deep Water. Of this 8 Sv, 3 Sv upwell to the upper layers mixing with Intermediate Water and 5 Sv return to the Circumpolar. In the South Pacific, the vertical change in upwelling forces an additional 4 Sv of Circumpolar Bottom Water to enter the western boundary current and an additional 2.5 Sv to return with the Deep Water. Thus, 12 Sv of Circumpolar Bottom Water enter the western bottom boundary current and 7.5 Sv of Pacific Deep Water return in the western deep boundary current. These values are comparable with estimates of the geostrophic calculations from SCORPIO data when the level of no motion is chosen near the benthic front (Warren and Voorhis, 1970). Overall, 14.5 Sv enter and leave the abyssal Pacific basin, giving 700 years for the residence time of the water.

Acknowledgments. I am grateful to G. Ostlund for letting me use the vertical sections of C-14 and to the staff of GOG for technical assistance. This work was funded by NSF grant OCE77-23093.

REFERENCES

Craig, H., Y. Chung and M. Fiadeiro. 1972. A benthic front in the South Pacific. Earth Planet. Sci. Lett., *16,* 50–65.

Fiadeiro, M. E. 1980. The alkalinity of the deep Pacific. Earth Planet. Sci. Lett., *49,* 499–505.

Fiadeiro, M. E. and H. Craig. 1978. Three-dimensional modeling of tracers in the deep Pacific Ocean: I. Salinity and oxygen. J. Mar. Res., *36,* 323–355.

Fiadeiro, M. E. and G. Veronis. 1977. On weighted-mean schemes for the finite-difference approximation to the advection-diffusion equation. Tellus, *29,* 512–522.

Kuo, H. H. and G. Veronis. 1973. The use of oxygen as a test for an abyssal circulation model. Deep-Sea Res., *20,* 871–888.

Munk, W. 1966. Abyssal recipes. Deep-Sea Res., *13,* 707–730.

Ostlund, H. G., R. Brescher, R. Oleson and M. J. Ferguson. 1979. GEOSECS Pacific radiocarbon and tritium results. Tritium Laboratory Data Report No. 8, Rosenstiel School of Marine and Atmospheric Sci., University of Miami, Florida.

Ostlund, H. G. and M. Stuiver. 1980. GEOSECS Pacific radiocarbon. Radiocarbon, *22,* 25–53.

Stommel, H. and A. B. Arons. 1960. On the abyssal circulation of the world. Part I—Stationary planetary flow patterns on a sphere. Deep-Sea Res., *6,* 140–154.

Warren, B. A. and A. D. Voorhis. 1970. Velocity measurements in the deep western boundary current of the South Pacific. Nature, *228,* 849–850.

Wyrtki, K. 1961. The thermohaline circulation in relation to the general circulation of the oceans. Deep-Sea Res., *8,* 39–64.

Received: *18 May, 1981;* revised: *1 March, 1982.*